Surface & Coatings Technology 480 (2024) 130601

Contents lists available at ScienceDirect

Surface & Coatings Technology

journal homepage: www.elsevier.com/locate/surfcoat

Full length article

Oxidation behavior of Ti_2AlC MAX phase-based coating on a γ-TiAl alloy TiAl48-2-2 produced by DC magnetron sputtering

Nadine Laska [a,*], Radosław Swadźba [b], Peter Nellessen [a], Oliver Helle [a], Ronja Anton [a]

[a] German Aerospace Center, Linder Hoehe, 51147 Cologne, Germany
[b] Łukasiewicz Research Network – Uppersilesian Institute of Technology, K. Miarki 12-14, Gliwice, Poland

ARTICLE INFO

Keywords:
Ti_2AlC MAX-phase
DC magnetron sputtering
γ-TiAl alloy TiAl48-2-2
Cyclic oxidation behavior

ABSTRACT

The application of intermetallic γ-TiAl-based alloys is limited by the deterioration in strength and creep resistance as well as reduction in oxidation resistance above 750 °C. The deposition of protective coatings is a promising opportunity to enhance the oxidation resistance or the lifetime with regard to the sustainability by several orders of magnitude. Moreover, additive manufacturing processes could enable the production of components with more complex geometries in the future. Thus, designs of γ-TiAl turbine blades with internal cooling systems could be feasible in the near future. In this context, the deposition of thermal barrier coatings and, therefore, oxidation protective bond coatings became important. MAX phases are of increasing interest as coating materials for high temperature applications due to their unique combination of metallic and ceramic properties. Especially the alumina forming MAX phases such as Cr_2AlC, Ti_2AlC or Ti_2AlN are promising coating materials.

In the present work a Ti_2AlC MAX-phase based coating was deposited by DC magnetron sputtering. Using three pure elemental target materials - Ti, Al and C and a two-fold rotation, a homogenous all-around coating was applied on the γ-TiAl alloy TiAl48-2-2 with a coating thickness of 10 µm. After the deposition process the stochiometric Ti_2AlC coating was X-ray amorphous, therefore a post-heat treatment at 800 °C for 1 h was performed to achieve the desired hexagonal phase. Finally, the MAX-phase coated TiAl48-2-2 alloy was subjected to a cyclic oxidation test at 850 °C in laboratory air. The Ti_2AlC MAX-phase coated TiAl48-2-2 alloy exhibits an excellent oxidation behavior, due to the formation of a thermally grown alumina top layer with the desired hexagonal Ti_2AlC MAX-phase below. Extensive TEM analyses also showed the dependence of Al_2O_3 formation on post-heat treatment. θ-Al_2O_3 with a lower protective effect and the concomitant formation of TiN under the TGO was observed with post-heat treatment in Ar, while post-heat treatment in air lead to the formation of a protective α-Al_2O_3 layer.

1. Introduction

Titanium aluminides gained significant attention as advanced materials for turbine blades in high-temperature environments. These intermetallic compounds possess exceptional a comparatively to the common used Ni-based alloys a low density. Due to their high-temperature stability in conjunction with their good mechanical properties enables the utilization of γ-TiAl alloys as material for turbine blades e.g. in jet engines by *General Electric* in the last two stages of the low-pressure turbine [1,2]. However, their susceptibility to oxidation at elevated temperatures presents a challenge for their implementation at service temperatures above ~750 °C. To address this issue, researchers have explored various protective coating strategies to enhance the oxidation resistance of titanium aluminides, thereby extending the service life and efficiency of turbine blades. Protective coatings will play a key role in the future, especially when it comes to the sustainability of raw materials. Recent research dates demonstrate the high potential and therefore the opportunity to improve oxidation resistance by several orders of magnitude through the deposition of intermetallic coatings such as Al—Si [3–5] or Ti-Al-Cr [6–8]. Moreover, the so called "halogen-effect" by implementing halogens, especially fluorine, into the surfaces of TiAl alloys is a smart solution to enhance the service temperature and is proven by several publications [9–13].

In the future, the possibilities of additive manufacturing techniques could enable integration of internal cooling channels in turbine blades made of γ-TiAl alloys [14,15]. This would also demonstrate the

* Corresponding author.
E-mail address: nadine.laska@dlr.de (N. Laska).

https://doi.org/10.1016/j.surfcoat.2024.130601
Received 24 January 2024; Accepted 25 February 2024
Available online 28 February 2024

usefulness of depositing complete thermal barrier coating systems consisting of an oxidation protection layer as bond coating and a ceramic top layer of, e.g. state of the art yttrium-stabilized zirconium oxide as thermal barrier [16,17].

However, all the currently published investigations of coatings for γ-TiAl, as well as their surface modifications, like the halogen-effect, enhance the oxidation resistance, but deteriorate the mechanical properties, in particular the fatigue behavior, of such coated components. Intermetallic coatings on γ-TiAl show a low crack resistance due to the formation of brittle Al-rich TiAl, Laves- or Ti_5Si_3 phases. Therefore, the fatigue properties of coated TiAl components is reduced at room temperature as well as at elevated temperatures [18,19]. Moreover, the implementation of halogens into the surface of TiAl alloys leads to a significant reduction in the mechanical properties due to an oxygen induced surface embrittlement. Hereby, the selective formation of an Al_2O_3 TGO caused the formation of an Al-depleted zone consisting of the α_2-Ti_3Al phase below the TGO. Unfortunately, the high solubility of oxygen in the α_2-Ti_3Al phase is therefore the responsible factor for the detrimental surface embrittlement of the TiAl alloys [20,21].

In the present work the usage of the so-called MAX-phases with M = transition metal like Ti or Cr, A = Si or Al and X = C or N, as coating material for titanium aluminides could offer a promising alternative. MAX-phases show both, excellent oxidation resistance, the required ductility as well as a low solubility for oxygen [22–25]. Unfortunately, degradation of MAX-phases is observed when applied on various Ti- or Ni-based alloys caused by interdiffusion processes between coating and alloy leading to Al-depletion [26,27]. This kind of degradation is probably not observed when MAX-phases were applied on the comparative Al-rich γ-TiAl based alloys. The Al-gradient could lead to an outwards diffusion of Al from the substrate alloy into the coating and finally to a stabilization of a the thermally grown alumina layer with a stable MAX-phase below. Moreover, MAX-phases as coating material could prevent the deterioration of the mechanical properties, especially the fatigue behavior of such coated γ-TiAl components in contrast to the common protective intermetallic, but brittle, coatings. First studies show the potential of these alumina forming MAX-phases of Cr_2AlC or Ti_2AlC as coating material for a γ-TiAl-based alloy [28–30]. Due to the higher thermodynamic stability and chemical compatibility as already show in the previous works the present paper is focused in the Ti_2AlC MAX phase as protective layer on the alloy already used alloy TiAl48–2-2.

2. Experimental section

Using direct current magnetron sputtering (DCMS) the MAX phase-based coating with the stochiometric composition of Ti_2AlC (50Ti-25Al-25C in at. %) were deposited on the γ-TiAl alloy *TiAl48-2-2* with the nominal chemical composition of 48 at. % Ti and Al, as well as 2 at. % Nb and Cr. The substrate material was supplied by *GfE–Gesellschaft for Elektrometallurgie, Nuremberg, Germany*. From the extruded and annealed *TiAl48-2-2* rods, disc-shaped specimens with 15 mm diameter and 1 mm thickness were machined by electrical discharge machining (EDM). The surfaces of the TiAl specimens were vibratory polished to a surface roughness below S_a = 1.6 μm and finally ultrasonically cleaned in ethanol.

The Ti_2AlC coatings were deposited by using three pure, elemental targets of Ti, Al and C in a multisource sputter coater (*IMPAX 1000 HT system by SVS Vacuum Coating Technologies, Karlstadt, Germany*), wherein up to four different target sources can be used. The low sputtering rate of C was compensated by spacing the TiAl48-2-2 samples as close as possible to the C target, while the Ti and Al targets were placed laterally. During the deposition process, the TiAl samples were rotated two-fold by a planetary gear to generate a homogeneous bilateral deposition. A schematic of the multisource sputtering machine is shown in Fig. 1.

An additional heating of the coating chamber was not applied during the sputtering process, the obtained substrate temperature was self-

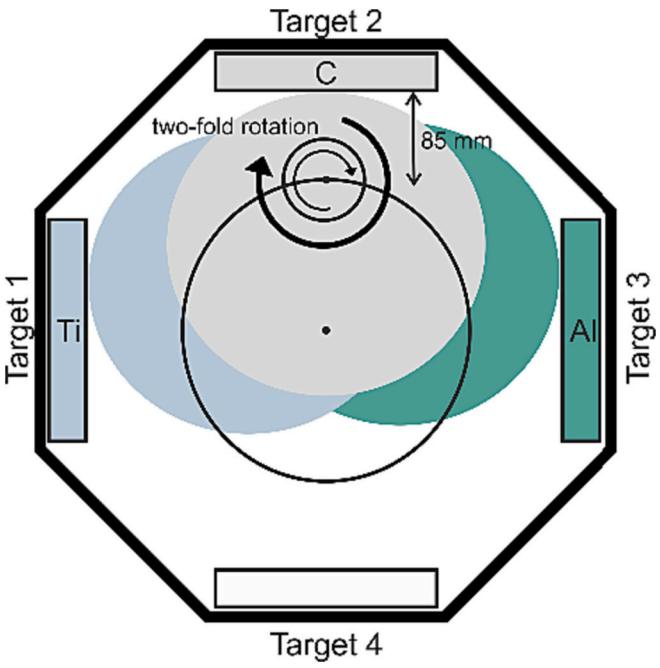

Fig. 1. Schematic of the multisource sputtering facility using DC magnetron sputtering to deposit the Ti_2AlC MAX phase-based coating on the γ-TiAl alloy TiAl48-2-2.

adjusted by the process conditions. Prior to the coating deposition, an Ar-plasma etching process for surface cleaning using a bias voltage of 500 V and a frequency of 100 kHz was carried out for 15 min. The system was operated with DC voltage and Ar was used as process gas. The sputtering parameters during the Ti_2AlC coating process are summarized in Table 1. The chemical composition of the achieved Ti-Al-C coating were measured by glow-discharge spectroscopy (GD-OES).

A post heat-treatment at 800 °C for 1 h was performed, to provide a fully crystalline microstructure of the Ti_2AlC MAX-phase-based coating. One the one hand a post heat-treatment was carried out under isothermal conditions in an Ar atmosphere using a heating rate of 400 °C/h. Before the oven was heated up, it was purged three times with Ar. In addition, a post heat-treatment in dry laboratory air was carried out under similar conditions. After the one-hour annealing, the furnaces were switched off and the samples were left to cool down in the oven.

Finally, the oxidation behavior of the Ti_2AlC coating on the TiAl48-2-2 alloy was tested in a fully automatic furnace cycle test rig at a calibrated temperature of 850 °C in laboratory air. Each cycle consisted of 60 min of heating followed by 10 min of cooling assisted by fans to nearly room temperature.

Metallographic cross sections of the coated specimens were prepared and analyzed with scanning electron microscopy (SEM) using a *DSM Ultra 55, Carl Zeiss NTS, Wetzlar, Germany* equipped with energy-dispersive X-ray spectroscope (EDS) by *Aztec, Oxford Instruments, Abingdon, UK*. All SEM images were taken with a secondary electron detector at 5 kV. The EDS measurements were carried out at 15 kV using a working distance of 8.5 mm.

A *FEI Helios NanoLab 600i* focused Ion Beam/Dual Beam (FIB/SEM) equipped with UltraDry energy-dispersive X-ray spectroscope (EDS)

Table 1
Sputtering parameters for the production of the Ti_2AlC MAX phase-based coating.

Target power [W]			p [mbar]	$T_{Substrate}$ [°C]	Ar [ml/min]	Sputter rate [μm/h]
Ti	Al	C	5.9×10^{-3}	230	300	1.25
4800	3800	1150				

from *THERMO FISHER SCIENTIFIC* was used for FIB lamella preparation. The high-resolution investigations of the coatings were performed using scanning transmission electron microscope (STEM) *FEI TITAN 80–300* operating at 300 kV with *Z*-sensitive high angle annular dark field (HAADF) and annular dark field (ADF) detectors. Both systems allowed a chemical analysis by energy-dispersive X-ray spectroscopy (EDS).

In order to analyze the phase formation after deposition and cyclic oxidation tests, X-ray diffraction was performed using a *Bruker D8 Advance* (Cu Kα radiation, *EVA/Topas 4.2 software package, Bruker AXS, Karlsruhe, Germany*).

3. Results

3.1. The as-coated state of the Ti_2AlC coating produced by DC magnetron sputtering

The Ti_2AlC coatings with a thickness of 10 µm produced by DC magnetron sputtering show good adhesion on the TiAl48-2-2 substrates. The SEM cross section, presented in Fig. 2a, shows a homogenous, slightly columnar coating morphology, typical for such PVD-based sputter layers. The quantitative, chemical composition was determined by a GD-OES depth profile, which is plotted in Fig. 2b.

The measured nominal chemical coating composition in at. % by GD-OES, neglecting the preliminary shifts during the initial measure progress due to impurities on the sample surface, is summarized in Table 2. In addition, the composition using EDS from the cross sections in the SEM is shown.

Since a quantitative analysis of carbon is difficult by both GD-OES and EDS due to impurities on the surface, the focus was on the ratio between Ti and Al. Here, a slightly higher Al-content in comparison to the stochiometric composition of the Ti_2AlC MAX-phase (with 50Ti-25Al-25C in at. %) was intended to compensate the expected Al-depletion in the coating, due to the formation of an alumina TGO, when exposed to high temperature environments.

The analysis of the sputter coating using X-ray shows an amorphous coating microstructure in the as-coated state, due to the low substrate temperature of 230 °C during the DCMS process, as already shown and discussed in previous work [28]. Therefore, the post heat-treatments was obligatory and performed at 800 °C for 1 h, as indicated by the results of *Abdulkadhim* et al. [31].

Table 2
Chemical composition of the Ti_2AlC coating on the TiAl48–2-2 alloy, measured by a GD-OES depth profile and EDS scan in at. % respectively.

Analytical method	Ti [at.%]	Al [at.%]	C [at.%]	Ti:Al ratio
GD-OES depth profile (average)	53	30	17	1.8
EDS scan	40	24	36	1.7

3.2. Post heat-treatments of the Ti_2AlC MAX phase-based coating on TiAl48-2-2 @ 800 °C for 1 h

The post heat-treatments were performed in an inert Ar-atmosphere, as well as in laboratory air at 800 °C for 1 h. The SEM cross sections of the Ti_2AlC MAX phase-based coating after these two different post heat-treatments are presented in Fig. 3.

The columnar coating morphology in the as-coated state was closed after the heat exposures and a homogeneous, dense, and well adherent Ti_2AlC coating on the TiAl48-2-2 alloy was achieved. In Fig. 3a, the heat-treated coating in an Ar atmosphere shows no formation of a TGO layer on the surface. Fig. 3b presents the SEM cross section of the Ti_2AlC coating after the exposition in laboratory air. Here, an additional thermally grown oxide (TGO) composed of a continuous alumina layer can be observed on top of the Ti_2AlC coating. The outer part of the oxide layer is composed of a mixture of alumina and titania. The thickness of the TGO is approximately 400 nm after 1 h at 800 °C.

The chemical composition of the Ti_2AlC coatings has not changed significantly in comparison to the as-coated state when considering the ratio of Ti and Al, measured by EDS in Table 3. The quantitative content of C is probably falsified by deposits on the surface and charging effects during the EDS measurements using SEM. The quantitative analysis by a GD-OES depth profile was not possible once an oxide layer on the surface is formed, due to the different excitation parameters of the ceramic TGO and the metallic coating materials below. The alloying elements Cr and Nb of the TiAl48-2-2 TiAl-based alloy were not detected by EDS in the Ti_2AlC coatings, therefore no interdiffusion processes between the coating and the TiAl48-2-2 alloy were observed after the post heat-treatments at 800 °C for 1 h. This was also confirmed by the chemical composition in the surface of the TiAl48-2-2 alloy.

For a more detailed analysis of the phase formations X-ray diffraction measurements were performed after the post heat-treatments in Ar as well as in lab air. The X-ray diffractograms are presented in Fig. 4. The XRD measurements confirm the formation of the desired Ti_2AlC MAX phase independent from the atmosphere during the post heat-

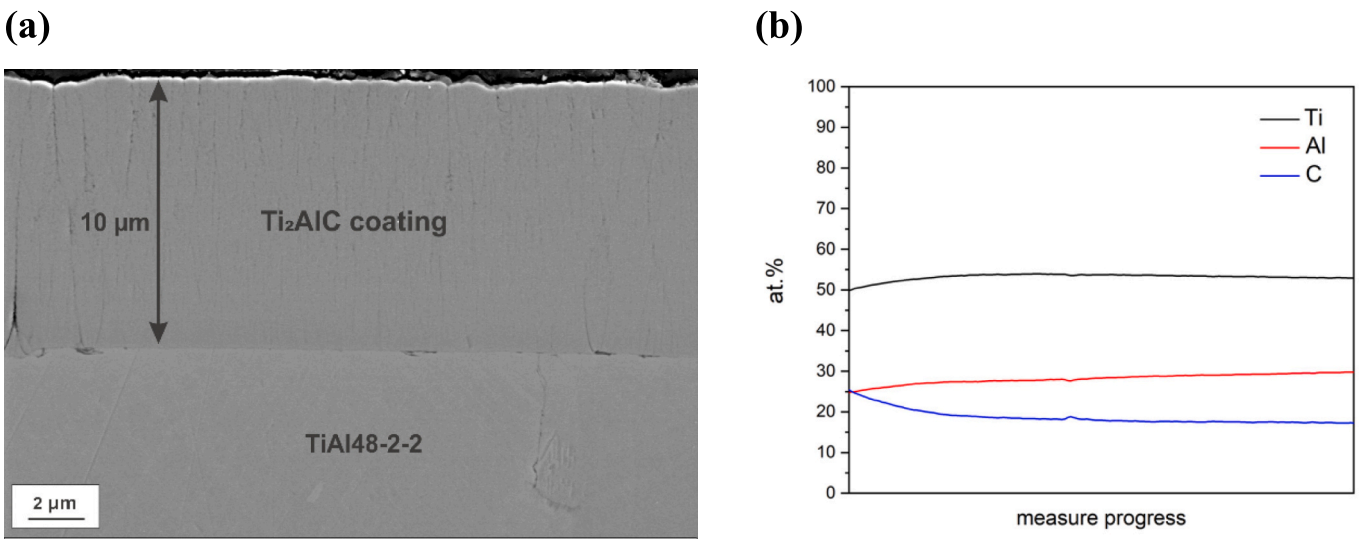

Fig. 2. SEM cross section of the Ti_2AlC coating after the deposition process using DC magnetron sputtering (a) and depth profile analysis using GD-OES of the chemical composition (b).

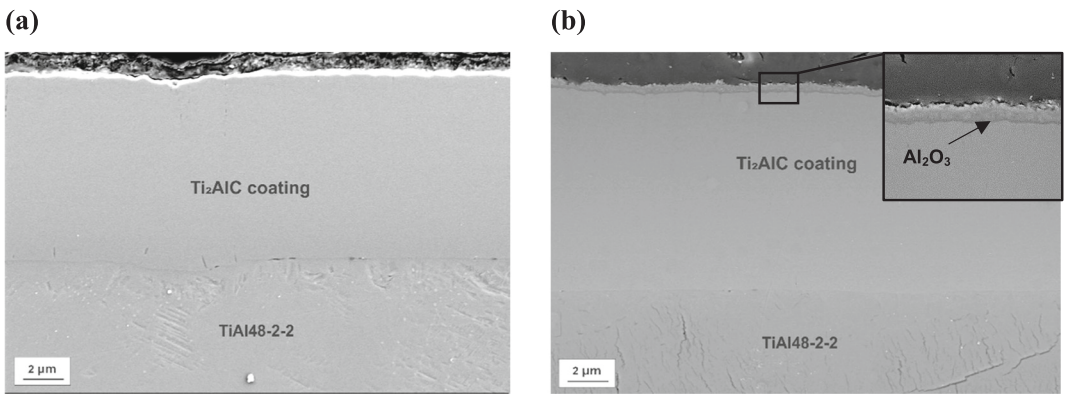

Fig. 3. SEM cross section of the Ti_2AlC coating after the post heat-treatment @ 800 °C for 1 h using an Ar-atmosphere (a) and dry laboratory air (b).

Table 3
Chemical composition of the Ti_2AlC coating on the TiAl48–2-2 alloy after the post heat-treatment in an Ar-atmosphere, as well as in dry laboratory air using EDS in at.%.

Atmosphere	Ti [at. %]	Al [at. %]	C [at. %]	TiAl ratio
Ar	40	24	37	1.7
lab air	35	21	44	1.7

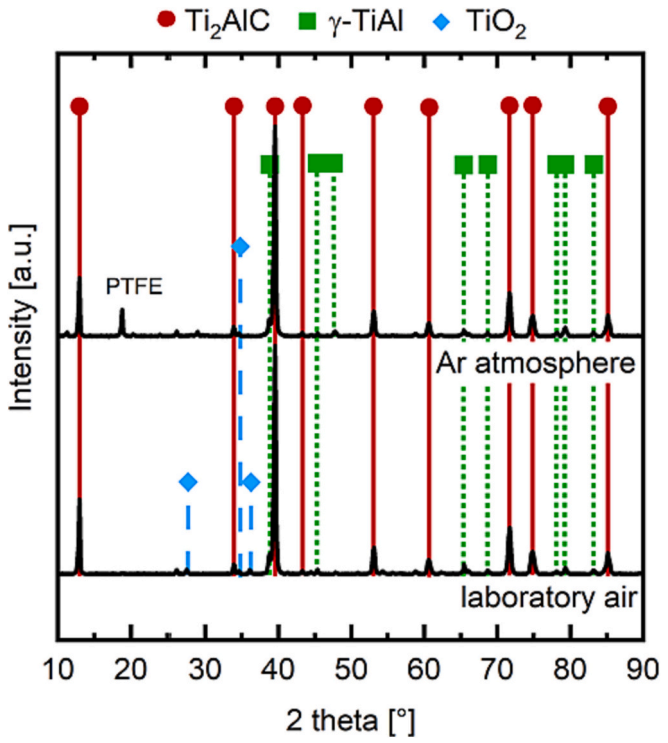

Fig. 4. X-ray measurement of the Ti_2AlC coating on TiAl48–2-2 after the post heat-treatment in an Ar-atmosphere and in laboratory air @800 °C for 1 h.

treatments. In particular the reflex at 13° is decisive for this. Reflections of the γ-TiAl phase can also be seen. The extent to which this phase is only present in the substrate or is also part of the layer cannot be clearly shown due to the used Bragg-Brentano geometry. In addition, the layer deposited in the Ar-atmosphere shows reflections that can possibly be assigned to TiO_2 (rutile). The reflection at approx. 20° can be attributed to the PTFE, which was used for the fixation of the sample.

3.3. Evaluation of the cyclic oxidation behavior of the Ti_2AlC coating on TiAl48-2-2 at 850 °C in laboratory air

Finally, the Ti_2AlC MAX-phase-based coating on the TiAl alloy TiAl48-2-2 was tested under cyclic conditions to simulate the near-application load in aircraft engines at 850 °C in laboratory air.

Fig. 5a presents the SEM cross section of the Ti_2AlC coating after heat-treatment at 800 °C in an Ar atmosphere followed by 20 1 h-cycles at 850 °C. The Ti_2AlC MAX phase coating formed a layer of pure aluminum oxide with a thickness of approximately 1 µm on the surface, showing good adherence, as well as a dense and homogenous microstructure. Above the dense TGO of pure alumina, a porous oxide layer of predominantly TiO_2 was observed, as shown in the EDS element mapping. A close up of the two-layered TGO is shown in Fig. 5a as well.

Below the TGO a homogenous coating was observed with a chemical composition of 38Ti-20Al-42C in at. % measured by EDS. The elemental mapping using EDS shows minor diffusion of Cr and Nb from the TiAl48-2-2 substrate material into the coating but could not be measured quantitatively by EDS. Niobium shows a homogenous distribution in the overall Ti_2AlC coating, while Cr shows a slight enrichment as a continuous layer in the lower part of the coating in conjunction with a visible Al-enrichment in the same region.

Fig. 5b shows the SEM cross section of Ti_2AlC coating on TiAl48-2-2 after post-heat treatment in Ar-atmosphere for 1 h at 800 °C followed by 50 1 h-cycles of exposure at 850 °C. The coating is already completely oxidized and a mixed oxide layer of TiO_2 and Al_2O_3 was formed. The Ti_2AlC MAX-phase is completely dissolved and horizontal cracks in the oxide layer show the onset of degradation of the coating by initial spallation from the TiAl48-2-2 alloy. Moreover, the surface of the TiAl48-2-2 alloy presents the formation of a TiO_2/Al_2O_3 mixed layer, similar like on uncoated TiAl-alloys presented in previous works [6].

The degradation mechanisms of the Ti_2AlC layer on the TiAl48-2-2 alloy were analyzed in more detail using TEM. For this purpose, a thin lamella was prepared using focused ion beam (FIB) technique from the cross-section of the Ti_2AlC coating heat treated in Ar atmosphere (Fig. 5a) after 20 1 h-cycles at 850 °C.

Fig. 6 shows the results obtained using STEM mode in conjunction with an EDS element mapping of the interface between the alumina layer and Ti_2AlC MAX phase coating. Below the alumina layer, an Al-depleted and N-enriched zone of about 100 nm was observed after 20 1 h-cycles at 850 °C in air, indicating the inwards diffusion of nitrogen in the Ti_2AlC coating. Moreover, at the grain boundaries of the Ti_2AlC MAX phase the depletion in Al is visible in addition to the presence of Cr. Chromium has diffused from the TiAl-48-2-2 substrate material through the whole Ti_2AlC coating to the TGO interface and precipitated predominantly at the grain boundaries in the coating, while in the TGO no significant Cr-enrichment could be observed. Niobium, which is also part of the substrate alloy could not detect in the upper part of the coating. Titanium and carbon were distributed homogenously in the

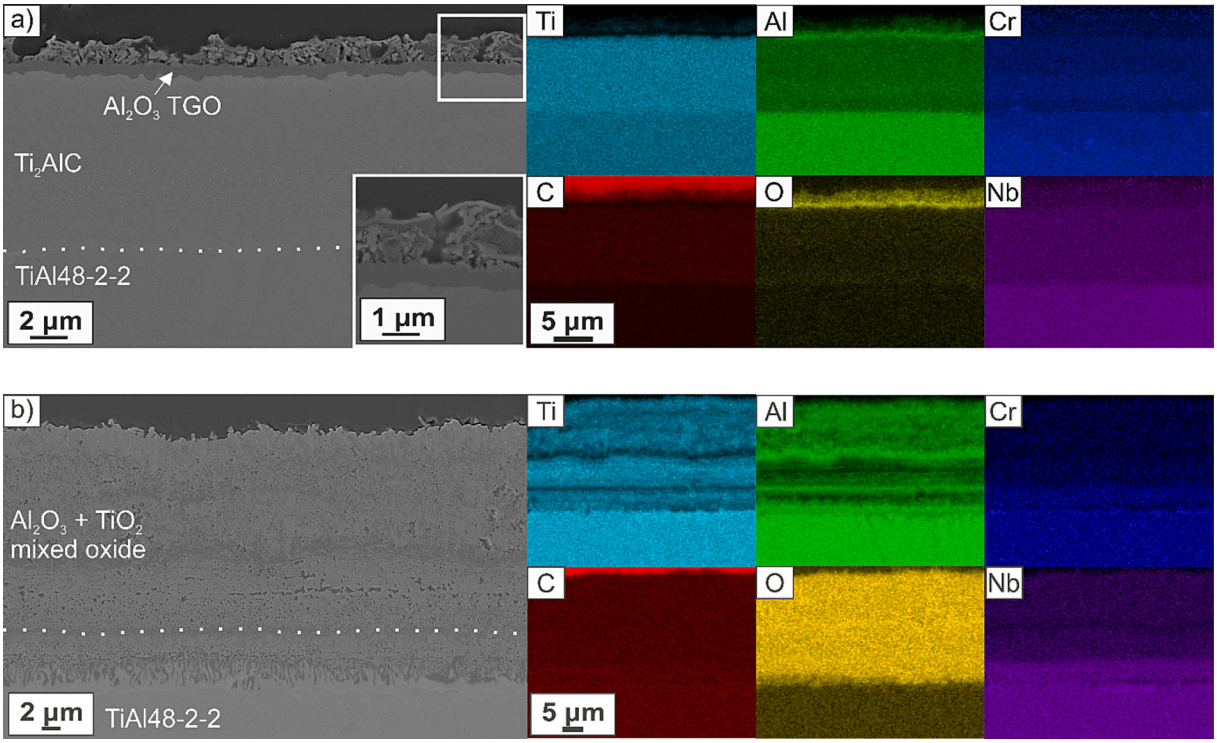

Fig. 5. SEM cross sections of the Ti_2AlC coating on the TiAl48–2-2 alloy with associated EDS element mappings after a post heat-treatment in Ar atmosphere for 1 h at 800 °C and the cyclic oxidation test for 20 (a) and 50 (b) 1 h-cycles at 850 °C in dry lab air.

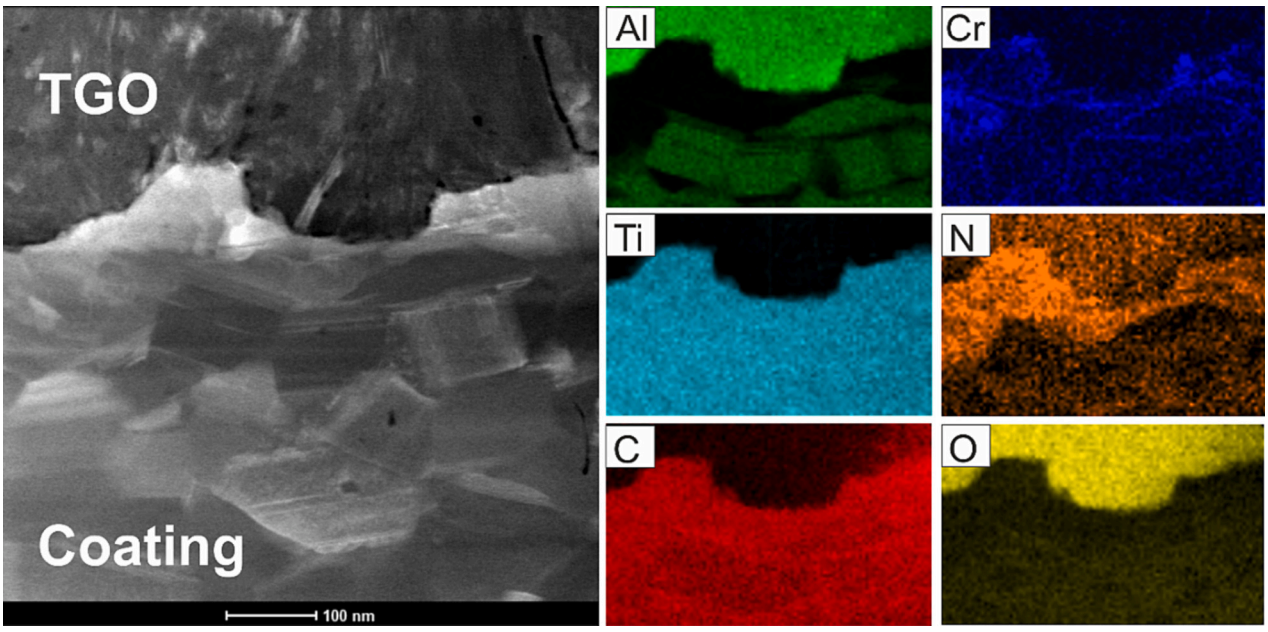

Fig. 6. STEM results of the TGO of alumina and Ti_2AlC coating interface with EDS element mappings by a FIB lamellar from Fig. 5a.

Ti_2AlC coating below the alumina layer.

By using the high-resolution TEM (HRTEM) along with selected area diffraction (SAD) and fast Fourier transform (FFT), shown in Fig. 7, the alumina layer on the surface could identified as theta-Al_2O_3, a transition metastable polymorph. Moreover, the N-enriched layer below the alumina layer was determined to be TiN, which indicates the inwards diffusion of nitrogen from the atmosphere into the surface.

Furthermore, the analysis using STEM with EDS elemental mappings of the Ti_2AlC coating below the TiN layer reveals a homogenous distribution of all measurable elements, presented in Fig. 8. The STEM image reveals a homogenous and fine-grained microstructure with grain sizes of <500 nm.

By the means of TEM bright field imaging along with HRTEM and SAD (Fig. 9a) it was demonstrated that the main part of the coating consists of the desired hexagonal Ti_2AlC MAX phase (Fig. 9b). In additions, the HRTEM (see Fig. 9c) shows the unique nanolaminate structure of this hexagonal Ti_2AlC MAX phase on the TiAl alloy TiAl48-2-2 after the cyclic oxidation test at 850 °C.

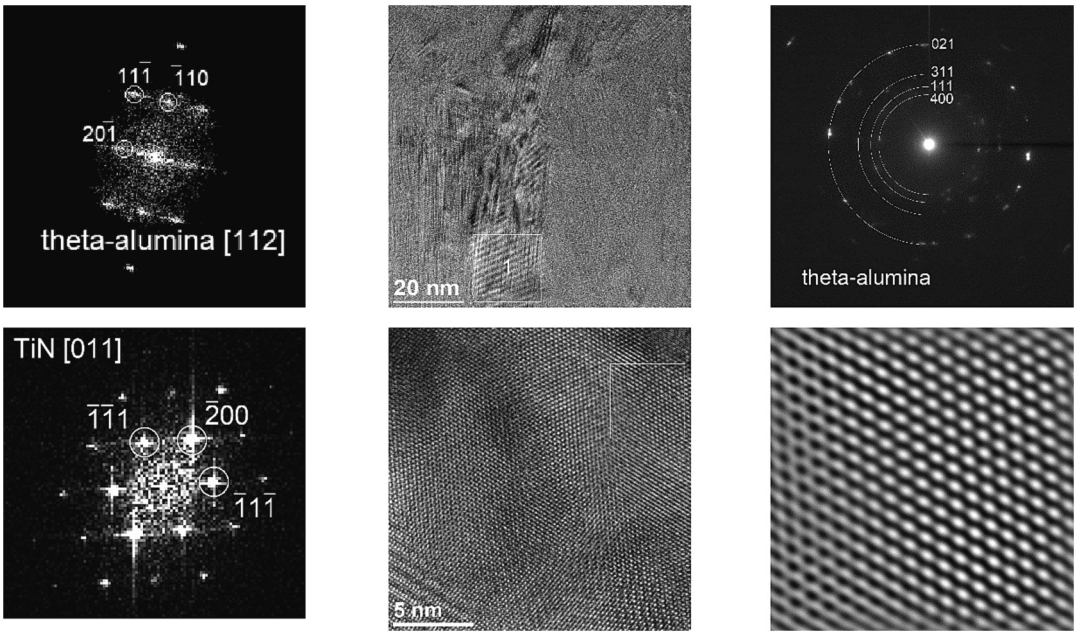

Fig. 7. HRTEM along with Fast Fourier Transform (FFT) and Selected Area Diffraction (SAD) images of the TGO with theta-Al_2O_3 and underlying TiN layer on the Ar heat-treated Ti_2AlC coating on TiAl48–2-2 alloy after 20 1 h-cycles at 850 °C in lab air.

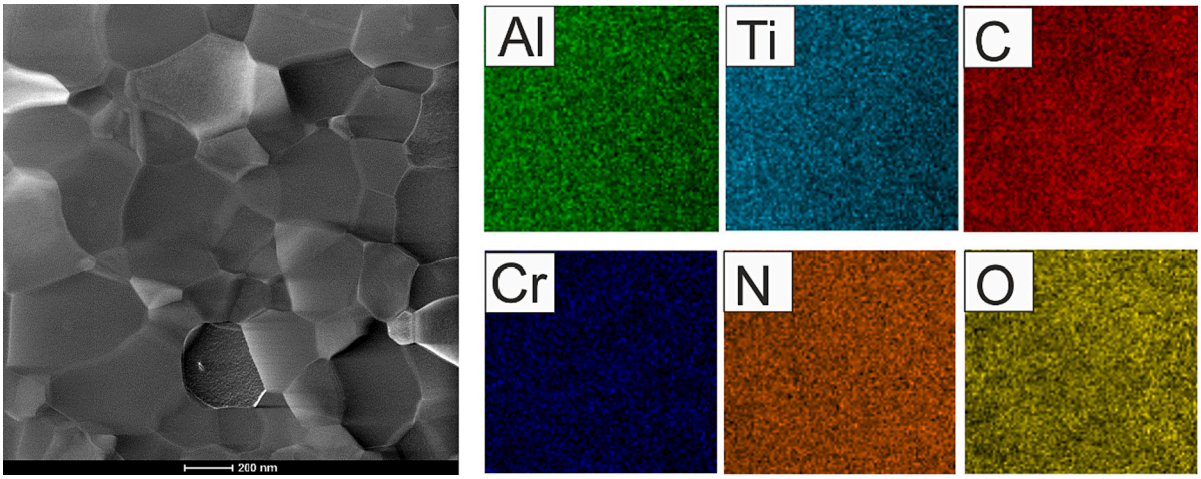

Fig. 8. STEM results of the Ti_2AlC coating on TiAl48–2-2 after 20 1 h-cycles at 850 °C (Fig. 5a) with EDS elemental mappings.

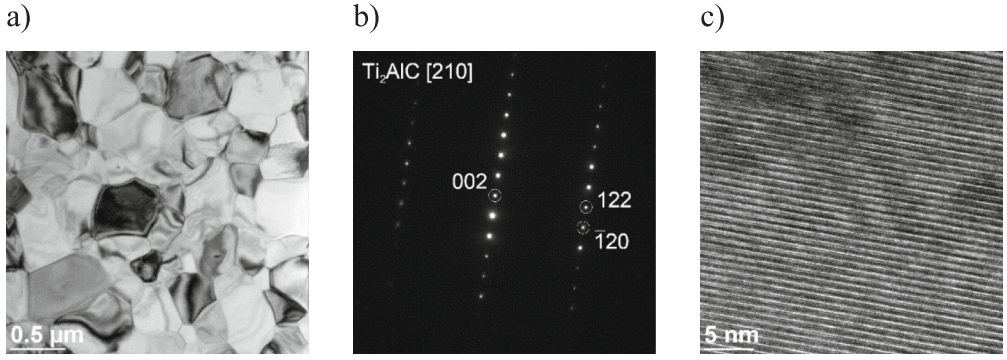

Fig. 9. Bright field (a), SAD (b) and HRTEM (c) images of the Ti_2AlC MAX-phase on the TiAl48-2-2 alloy after 20 1 h-cycles of exposure to 850 °C in air.

In the lower part of the coating, near to the interface with the TiAl48-2-2 substrate alloy some small Al- and Cr-rich precipitates were observed, formed by the outwards diffusion of Cr and Al from the TiAl48-2-2 alloy into the Ti_2AlC coating. Using HRTEM in conjunction with SAD, these precipitates were identified as the hexagonal $CrAl_2$ phase (see Fig. 10).

Finally, the Ti_2AlC coating on TiAl48-2-2 were post heat-treated in laboratory air for 1 h at 800 °C and afterwards tested under cyclic oxidation conditions. Fig. 11 presents SEM cross sections with associated EDS element mappings of the Ti_2AlC coating after 100 1 h-cycles of exposure to 850 °C in laboratory air.

Below a thin TGO of pure alumina a homogenous coating consisting of the Ti_2AlC MAX phase was observed by using SEM after 100 1 h-cycles of exposure. The thickness of the TGO only increased slightly by around 1 μm. After 100 1 h-cycles the TGO consists of two layers similar like on the post heat-treated Ti_2AlC coating in Ar-atmosphere (shown in Fig. 5a). The outer oxide layer is interspersed by TiO_2 but is significantly thinner and less porous compared to the layer shown in Fig. 5a. The continuous inner TGO of pure alumina shows a dense and homogenous microstructure with a thickness of about 500 nm.

However, in general, the Ti_2AlC coating shows a good oxidation protection for the TiAl48-2-2 alloy, when a post heat-treatment in dry laboratory air is performed.

XRD measurements at room temperature after different cycles of exposure to 850 °C confirm the stable formation of the desired hexagonal Ti_2AlC MAX-phase on the TiAl alloy TiAl-48-2-2 next to Al_2O_3 up to the in the present work performed total exposure time of 100 1 h-cycles at 850 °C. Moreover, the XRD measurement presents the formation of the stable polymorph of α-Al_2O_3 directly after the first 20 1 h-cycles up to the total testing time. Some minor reflections of TiO_2 (rutile) were also visible after 20 and 50 1 h-cycles. After 100 1 h-cycles TiO_2 could not detected anymore probably due to spallation of the outer TGO. However, this does not matter with regard to a long service life due to the protective Al_2O_3 layer. The X-ray diffractions after the post heat-treatment in air again for comparison, as well as after 20,50 and 100 1 h-cycles of exposure to 850 °C are presented in Fig. 12.

4. Discussion

In the present study it could be shown, that physical vapor deposition (PVD) techniques, especially direct current magnetron sputtering (DCMS) can be used for the manufacturing of MAX phase-based Ti_2AlC coatings. A film thickness of 10 μm could be obtained, which enables the application of the MAX phases as protective coating material for high temperature applications [6,32]. The utilization of DCMS using three pure elemental targets of Ti, Al and C could compensate the low sputter rate of C by placing the rotating components directly in front of the C target. This sample arrangement in the coating chamber by a lower distance between samples and C source increased the coating deposition rate by about 30 % compared to the previously published work [28], where a coating thickness of just 7 μm was achieved by the utilization of two C-sources in the opposite directions using the same multisource sputter facility (Fig. 1). Moreover, the high flexibility due to the three separate elemental targets enable the optimization if the initial chemical composition of the coating in the as-coated state. Moreover, an initial higher amount of Al could be made possible, which is suitable and can compensate the later formation of the protective TGO of alumina. The achieved nominal chemical composition of 53Ti-30Al-17C (in at. % measured by GD-OES) with a significantly higher Al amount than the stochiometric Ti_2AlC MAX phase is optimized for the formation of the hexagonal Ti_2AlC MAX-phase in conjunction with a TGO of pure and therefore protective alumina on the surface. The slightly lower C content could not be optimized even by changing the GD-OES measurement parameters and calibrations several times. However, in conjunction with the other analytical methods used, in particular X-ray spectroscopy after the post-heat treatments, a layer composition close to the Ti_2AlC MAX phase can be assumed.

The initial slightly columnar structure of the Ti_2AlC coating corresponds to the well-known structural zone model by Thornton [33,34]. The low process temperature was not sufficient to form a crystalline microstructure at the self-adjusted substrate temperature by the target powers of 230 °C (Table 1) without any further heating or a substrate bias voltage. Therefore, the obtained layer was X-ray amorphous after fabrication process via DCMS due to a to low adatom mobility during the coating growth. For high temperature application, a subsequent heat treatment processes themes essential to densify the layer morphology on the one hand and to form a crystalline MAX phase in the coating with a TGO of pure alumina on the surface on the other hand.

4.1. Phase development of the Ti_2AlC coating by heat treatments @800 °C for 1 h in different atmospheres

The post heat-treatments in an inert Ar-atmosphere, as well as in dry laboratory air were carried out at 800 °C for 1 h to obtain the desired hexagonal Ti_2AlC MAX phase in accordance with the already published work by *Abdoulkadhim* et al. [31]. Hereby, the reflex of the [002] lattice plane at 13° in the XRD results is crucial for proving the formation of the Ti_2AlC MAX phase. Using an Ar-atmosphere, as well as dry lab air the formation of the desired hexagonal Ti_2AlC phase could observed by the X-ray measurements shown in Fig. 4. The remaining reflections could be assigned here at the γ-TiAl phase, which is part of the substrate material and were probably co-detected by using the Bragg-Brentano arrangement.

The post heat-treatment in Ar-atmosphere enables the development of the Ti_2AlC MAX-phase on the TiAl48-2-2 alloy independent from any oxidation processes. The coating provides a homogenous and dense morphology after the heat treatment at 800 °C for 1 h as required, without any noteworthy interdiffusion between the coating and the

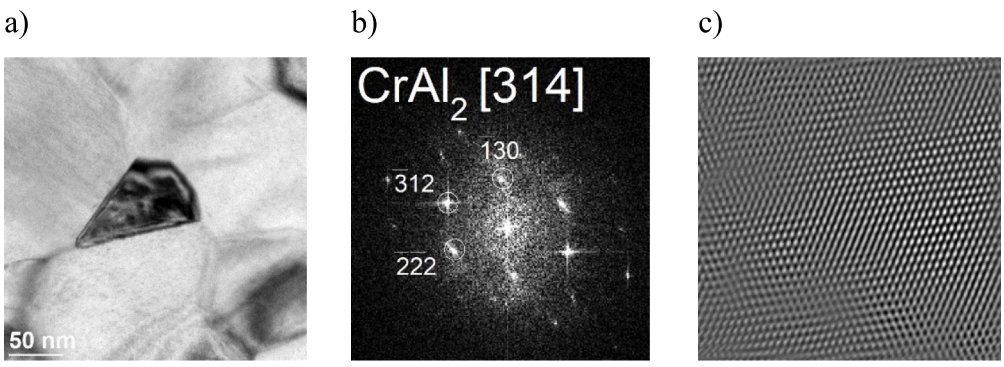

Fig. 10. Bright field (a), FFT (b) and HRTEM (c) images of the Cr_2Al phase at the lower part of Ti_2AlC MAX-phase on the TiAl48-2-2 alloy after 20 1 h-cycles of exposure to 850 °C in air.

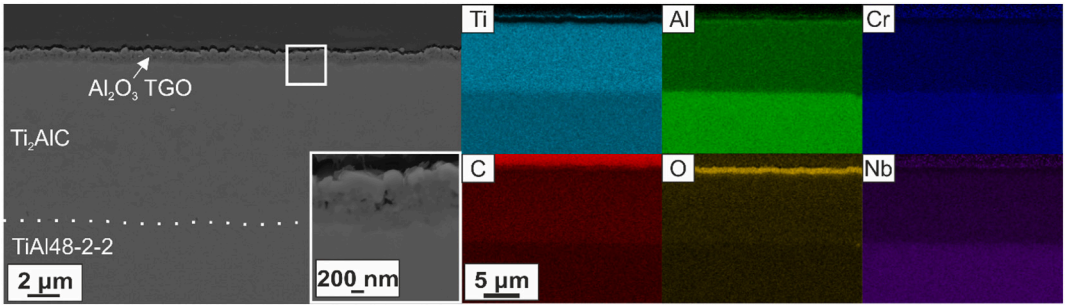

Fig. 11. SEM cross sections of the Ti_2AlC coating on the TiAl48–2-2 alloy with associated EDS elemental mappings after a post heat-treatment in laboratory air for 1 h at 800 °C and a cyclic oxidation test at 850 °C for 100 1 h-cycles in dry lab air.

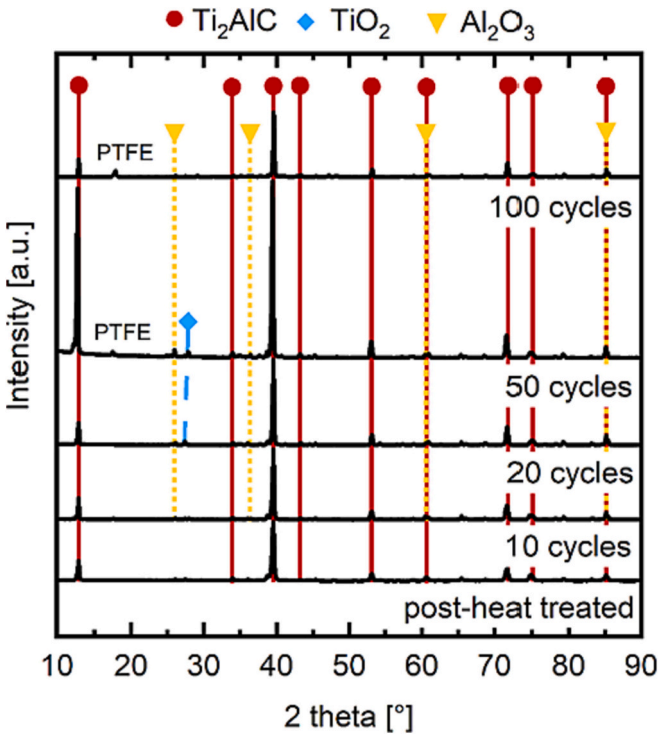

Fig. 12. X-ray diffractions of the Ti_2AlC coating on TiAl48–2-2 alloy heat treated for 1 h at 800 °C in air after 0, 10, 20, 50 and 100 1 h cycles at 850 °C in dry lab air. The measurements were performed at RT.

substrate alloy.

During the exposure to laboratory air the simultaneous formation of the Ti_2AlC MAX phase and a thin TGO on the coating surface occurs. The analysis of the TGO was difficult due to the low thickness of the oxide layer, but the XRD measurements show the presence of TiO_2 reflections, while the analysis of the cross section by SEM suggests a closed and pure alumina oxide layer with mixture of TiO_2 and Al_2O_3 above, see Fig. 3b. The ratio of Ti:Al (measured by EDS in SEM) in the film did not change in either case of post heat-treatment. Previous consideration suggested the assumption, that a simultaneous formation of MAX-phase and TGO from an amorphous material could lead to an advanced development of TiO_2 on the surface, due to the high Ti content in comparison to the Al content in the Ti_2AlC coating. As mentioned in the introduction only MAX-phases (with A = Al) can enable the formation of pure alumina layer as TGO's with an Al-content of just 25 at. %, due to their unique combination of the different bonding types in the crystal structure and therefore the minor binding enthalpy of Al in the MAX phases with A = Al. The outer part of the TGO, which consists mainly of TiO_2 could thus have been formed by oxidation of the Ti-rich amorphous layer, while Al_2O_3 could have been formed after crystallization and thus the formation of the MAX phase (Fig. 3b).

Basically, the crystalline Ti_2AlC MAX phase as coating material provides a good adhesion due to the similar coefficient of thermal expansion (CTE) in comparison to the γ-TiAl-based alloy TiAl48-2-2. The low difference in the CTE is in the same order of magnitude just of 1-2 * 10-6 (K-1) [35,36].

4.2. Cyclic oxidation behavior of the Ti_2AlC MAX phase-based coating on the TiAl48-2-2 alloy

The Ti_2AlC MAX-phase develops the desired, thin TGO of predominantly alumina during the cyclic oxidation tests at 850 °C in dry laboratory air, when a post heat-treatment in either Ar-atmosphere or lab air for 1 h at 800 °C was performed. However, when heat treated in Ar, the Ti_2AlC coating provides an inferior oxidation behavior, probably due to the formation of a TGO consisting of the metastable polymorph of θ-Al_2O_3 as proven by TEM analysis (Fig. 7). This fast-growing and non-protective polymorph θ-Al_2O_3 cannot provide a sufficient oxidation protection due to its pseudo-cubic defect spinel structure as already published in previous works [37–39]. In particular the inferior protective properties of θ-Al_2O_3 for TiAl-based alloys is already published in previous works [40,41]. Here, the minor oxidation behavior is proven by significantly higher mass gain during the high temperature exposure.

One suggestion is a support of the formation of θ-alumina by a low residual oxygen content in the tube furnace during the post heat-treatment in the Ar-atmosphere, although no oxide layer was visible in the SEM cross section, see Fig. 3a. However, this could be due to a poor preparation of the cross section, as a gap has formed between the layer and the embedding material. Previous research word by *Swadzba* et al. have already shown that a lower oxygen content leads to the formation of metastable oxides θ-Al_2O_3 [42,43]. The growth of the TGO during the further cyclic oxidation tests could be influenced by the initial growth of a cubic spinel structure.

Below the alumina TGO formed on the Ar heat treated coating, the formation of TiN could be observed by analytical STEM method after 20 1 h-cycles at 850 °C, see Fig. 6. The formation of the TiN phase at the interface between the TGO and Ti_2AlC layer also proves that nitrogen must have diffused through the Al_2O_3 layer into the coating. Accordingly, the formed TGO shows also no barrier for nitrogen. TiN oxidizes rapidly to TiO_2 during longer exposure times in air and therefore has a negative effect on the oxidation behavior, as has already been shown in previous works [44]. In addition, the formation of nitrides should be avoided, particularly with regard to the mechanical properties of such coated components. Further TEM investigations must show the extent to which this diffusion of nitrogen did not occur in the layer post-treated in air.

Moreover, it is also thinkable that the rapid oxidation during the cyclic exposure with a heating rate of just a view seconds up to 850 °C is responsible for inferior oxidation behavior of the crystalline, but bare Ti_2AlC MAX phase. The post heat-treatment in air could lead as a kind of

pre-oxidation and therefore to a more subtle and stable conditions and therefore to the formation of a protective TGO of α-Al_2O_3.

However, below the surface layer zone the presence of a nearly homogeneous coating composed of the desired hexagonal Ti_2AlC MAX phase was confirmed by TEM (Fig. 9). The homogeneous MAX phase zone extends over several μm and therefore once again demonstrates the promising approach of producing MAX phase-forming coatings for high-temperature applications using DCMS. The high resolution TEM images (Fig. 9c) show the unique nanolaminate structure of this Ti_2AlC MAX-phase.

In the lower coating area near to the interface of TiAl48-2-2 alloy, sporadic small precipitates of the Cr_2Al phase were observed. The Cr_2Al phase was formed due to the outwards diffusion of Cr from the TiAl48-2-2 substrate alloy into the coating. However, Nb containing phases could not be observed showing a lower diffusion rate of Nb from the TiAl48-2-2 alloy into the Ti_2AlC coating. Niobium is present in a low concentration dissolved in the crystal lattice or substituting Ti, as has already been observed for other intermetallic phases such as $TiCr_2$ Laves phases [16]. Further investigations utilizing long-term oxidation tests must show to what extent the Cr_2Al precipitates increase in size and what influence this has on the stability and finally the performance of the Ti_2AlC MAX phase-based coating as oxidation protective layer on TiAl-based alloys.

Finally, a post heat-treatment of the Ti_2AlC coating in lab air at 800 °C for 1 h and therefore the simultaneous formation of the MAX-phase with a thermally grown oxide layer of alumina on the surface shows a much better oxidation behavior during the subsequently performed cyclic oxidation tests at 850 °C. The formation of protective thermally grown α-Al_2O_3 on the alloy surface is probably responsible for this good oxidation behavior. The passivating polymorph α-Al_2O_3 provides a well-known protection due to the parabolic, diffusion-controlled growth rate, which is already well known also for FeCrAl or MCrAlY alloys and published previous works [45]. Moreover, the formation of α-Al_2O_3 could prevent the inwards diffusion of nitrogen and therefore the formation of a TiN layer below the TGO by its dense hexagonal closed packed crystal structure. However, further TEM investigations are necessary for a more detailed analysis of the TGO itself and the interface between alumina layer and Ti_2AlC MAX-phase layer, when a post heat-treatment in dry lab air for 1 h at 800 °C was performed. Nevertheless, the present results using SEM with EDS element mappings (Fig. 11) in conjunction with X-ray measurement (Fig. 12) after different numbers of 1 h-cycles at 850 °C up to the maximal tested time of 100 h. reveal the stable formation of protective α-Al_2O_3 as TGO with a apparently homogenous Ti_2AlC MAX-phase coating below on the TiAl-alloy TiAl48-2-2, which is promising for further applications in high temperature atmospheres.

5. Conclusions

The manufacturing process by direct current magnetron sputtering (DCMS) allows the production of MAX-phase based coatings with a thickness of 10 μm, which should be sufficient for high temperature applications. The Ti_2AlC MAX-phase applied as oxidation protective coating can provided a good oxidation behavior on the γ-TiAl-based alloy TiAl48-2-2 for up to 100 h. by cyclic exposure to 850 °C in dry laboratory air.

The performance of the Ti_2AlC MAX-phase based layer depends significantly on the formed TGO on the surface. The α-Al_2O_3 polymorph, which is known to be protective, could be formed by a subsequent heat treatment after the DCMS process in dry laboratory air at 800 °C for 1 h, whereas the similar heat treatment in an inert Ar-atmosphere leads to the formation of meta-stable θ-Al_2O_3 and therefore to a minor oxidation behavior during the afterwards performed cyclic oxidation tests at 850 °C. For practical application purposes, a heat treatment in air is preferable since it is simpler and less expensive.

CRediT authorship contribution statement

Nadine Laska: Conceptualization, Funding acquisition, Writing – original draft. **Radosław Swadźba:** Formal analysis, Visualization, Writing – review & editing. **Peter Nellessen:** Data curation, Formal analysis, Validation, Writing – review & editing. **Oliver Helle:** Methodology, Writing – review & editing. **Ronja Anton:** Formal analysis, Visualization, Writing – review & editing.

Declaration of competing interest

Nadine Laska reports financial support was provided by German Aerospace Center DLR. Nadine Laska reports a relationship with German Aerospace Center DLR that includes: board membership. If there are other authors, they declare that they have no known competing financial interests or personal relationships that could have appeared to influence the work reported in this paper.

Data availability

The authors do not have permission to share data.

Acknowledgment

The authors thank the German Federation of Industrial Research Associations (AiF) for funding this project (IGF grant 22355 N). Moreover, the authors thank J. Brien, F. Kreps and A. Ebach-Stahl for the scientific and technical support at the German Aerospace Center, as well as for comments that greatly improved the manuscript.

References

[1] B.P. Bewlay, et al., TiAl alloys in commercial aircraft engines, Mater. High Temp. 33 (4–5) (2016) 549–559.
[2] B.P. Bewlay, et al., The science, technology, and implementation of TiAl in commercial aircraft engines, in: MRS Proceedings, Cambridge University Press, 2013, p. 1516.
[3] P.-P. Bauer, N. Laska, R.J.I. Swadźba, Increasing the Oxidation Resistance of γ-TiAl by Applying a Magnetron Sputtered Aluminum and Silicon Based Coating 133, 2021, p. 107177.
[4] P.-P. Bauer, et al., Aluminum diffusion inhibiting properties of Ti5Si3 at 900° C and its beneficial properties on Al-rich oxidation protective coatings on γ-TiAl, Corros. Sci. 201 (2022) 110265.
[5] R. Swadźba, et al., Microstructure and cyclic oxidation resistance of Si-aluminide coatings on γ-TiAl at 850 °C, Surf. Coat. Technol. 403 (2020) 126361.
[6] N. Laska, R. Braun, S. Knittel, Oxidation behavior of protective Ti-Al-Cr based coatings applied on the γ-TiAl alloys Ti-48-2-2 and TNM-B1, Surf. Coat. Technol. 349 (2018) 347–356.
[7] R. Braun, et al., Oxidation Protection of γ-TiAl Alloys by Intermetallic Ti-Al-Cr-Zr Coatings. MRS Online Proceedings Library, 2013, p. 1516.
[8] R. Braun, F. Rovere, P.H. Mayrhofer, C. Leyens, Environmental protection of γ-TiAl based alloy Ti-45Al-8Nb by CrAlYN thin films and thermal barrier coatings, Intermetallics 18 (4) (2010) 479–486.
[9] A.Z. Donchev .H.-E., M. Schütze, The halogen effect for improving the oxidation resistance of TiAl-alloys, Mater. High Temp. 22 (2005) 309–314.
[10] R. Pflumm, S. Friedle, M. Schütze, Oxidation protection of γ-TiAl-based alloys–a review, Intermetallics 56 (2015) 1–14.
[11] P.J. Masset, M. Schutze, Oxidation tests with untreated and F-treated TNBV5 alloys, ECS Trans. 25 (25) (2010) 45–56.
[12] N. Laska, et al., Lifetime of 7YSZ thermal barrier coatings deposited on fluorine-treated γ-TiAl-based TNM-B1 alloy, Mater. Corros. 67 (11) (2016) 1185–1194.
[13] R. Pflumm, et al., High-temperature oxidation behavior of multi-phase Mo-containing γ-TiAl-based alloys, Intermetallics 53 (2014) 45–55.
[14] H.A. Soliman, M. Elbestawi, Titanium aluminides processing by additive manufacturing–a review, Int. J. Adv. Manuf. Technol. 119 (9–10) (2022) 5583–5614.
[15] J. Gussone, et al., Microstructure of γ-titanium aluminide processed by selective laser melting at elevated temperatures, Intermetallics 66 (2015) 133–140.
[16] N. Laska, R. Braun, Lifetime of thermal barrier coatings deposited on γ-TiAl based alloys using intermetallic Ti–Al–Cr bond coats with additions of yttrium and zirconium, Oxid. Met. 81 (1–2) (2014) 83–93.
[17] R. Braun, et al., Oxidation behaviour of TBC systems on γ-TiAl based alloy Ti–45Al–8Nb, Oxid. Met. 71 (5) (2009) 295–318.
[18] S. Guth, et al., Influence of oxidation protective SiAl coatings on the tensile and fatigue behavior of Ti–48Al–2Cr–2Nb at elevated temperatures, Mater. Sci. Eng. A 858 (2022) 144182.

[19] N. Laska, R. Braun, Oxidation and fatigue behaviour of gamma titanium aluminides coated with yttrium or zirconium containing intermetallic Ti–Al–Cr layers and thermal barrier coating, Mater. High Temp. 32 (1–2) (2015) 221–229.
[20] A. Straubel, et al., Mechanical properties and microstructure of a TNM alloy protected by the fluorine effect and coated with a thermal barrier, in: Gamma Titanium Aluminide Alloys 2014, John Wiley & Sons, Inc, 2014, pp. 105–109.
[21] X. Wu, et al., Oxidation-induced embrittlement of TiAl alloys, Intermetallics 17 (7) (2009) 540–552.
[22] J. Gonzalez-Julian, Processing of MAX Phases: From Synthesis to Applications 104 (2), 2021, pp. 659–690.
[23] J.L. Smialek, Oxidation of Al_2O_3 scale-forming MAX phases in turbine environments, Metall. Mater. Trans. A 49 (3) (2018) 782–792.
[24] M.W. Barsoum, MAX Phases: Properties of Machinable Ternary Carbides and Nitrides, John Wiley & Sons, 2013.
[25] O. Berger, et al., Characterization of Cr–Al–C and Cr–Al–C–Y films synthesized by high power impulse magnetron sputtering at a low deposition temperature, Thin Solid Films 580 (2015) 6–11.
[26] Q. Wang, et al., Fabrication and oxidation behavior of Cr_2AlC coating on Ti6242 alloy, Surf. Coat. Technol. 204 (15) (2010) 2343–2352.
[27] W. Garkas, M. Fröhlich, K.-D. Weltmann, C. Leyens, Oxidation and decomposition of Ti_2AlN MAX phase coating deposited on nickel-based super alloy IN718, Mater. Sci. Forum 825-826 (2015) 628–635.
[28] N. Laska, et al., Sputtering and characterization of MAX-phase forming Cr–Al–C and Ti–Al–C coatings and their application on γ-based titanium aluminides, Adv. Eng. Mater. n/a(n/a) (2021) 2100722.
[29] R. Mitra, et al., Study of Interfaces In XD TM Al/TiC p Metal Matrix Composites vol. 238, 1991.
[30] L. Mengis, et al., Synthesis, oxidation resistance and mechanical properties of a Cr2AlC-based MAX-phase coating on TiAl, Intermetallics 163 (2023) 108039.
[31] A. Abdulkadhim, et al., MAX Phase Formation by Intercalation Upon Annealing of TiCx/Al ($0.4 \leq x \leq 1$) Bilayer Thin Films 59(15), 2011, pp. 6168–6175.
[32] A. Ebach-Stahl, et al., Cyclic oxidation behaviour of the titanium alloys Ti-6242 and Ti-17 with Ti–Al–Cr–Y coatings at 600 and 700°C in air, Surf. Coat. Technol. 223 (0) (2013) 24–31.
[33] J.A. Thornton, The microstructure of sputter-deposited coatings, J. Vac. Sci. Technol. A 4 (6) (1986) 3059–3065.
[34] J.A. Thornton, High rate thick film growth, Annu. Rev. Mater. Sci. 7 (1) (1977) 239–260.
[35] M. Barsoum, et al., Processing and Characterization of Ti 2 AlC, Ti 2 AlN, and Ti 2 AlC 0.5 N 0.5 31(7), 2000, pp. 1857–1865.
[36] P. Bartolotta, et al., The Use of Cast Ti− 48Al− 2Cr− 2Nb in Jet Engines 49(5), 1997, pp. 48–50.
[37] A.H. Heuer, et al., Alumina scale formation: a new perspective, J. Am. Ceram. Soc. 94 (s1) (2011) s146–s153.
[38] G.C. Rybicki, J.L. Smialek, Effect of theθ-α-Al2O3 transformation on the oxidation behavior ofβ-NiAl + Zr, Oxid. Met. 31 (3) (1989) 275–304.
[39] J. Yang, et al., Transient oxidation of NiAl, Acta Mater. 46 (6) (1998) 2195–2201.
[40] V. Gauthier, et al., Oxidation-resistant aluminide coatings on γ-TiAl, Oxid. Met. 59 (3) (2003) 233–255.
[41] P.-P. Bauer, et al., Effect of Si content on deposition and high-temperature oxidation of Al-Si coatings obtained by magnetron sputtering PVD method, Coatings 12 (6) (2022) 859.
[42] R. Swadźba, et al., Effect of Pre-oxidation on Cyclic Oxidation Resistance of γ-TiAl at 900° C 177, 2020, p. 108985.
[43] F. Dettenwanger, et al., Microstructural study of oxidized γ-TiAl, Oxid. Met. 50 (3) (1998) 269–307.
[44] N. Zheng, et al., Studies concerning the effect of nitrogen on the oxidation behavior of TiAl-based intermetallics at 900°C, Oxid. Met. 44 (5–6) (1995) 477–499.
[45] H. Singh, et al., Characterisation of high temperature oxide scales for plasma sprayed NiCrAlY coated Ni-and Fe-based superalloys, Anti-Corros. Methods Mater. 53 (5) (2006) 283–295.